Host microRNA molecular signatures associated with human H1N1 and H3N2 influenza A viruses reveal an unanticipated antiviral activity for miR-146a

Olivier Terrier,[1] Julien Textoris,[2] Coralie Carron,[1] Virginie Marcel,[3] Jean-Christophe Bourdon[3] and Manuel Rosa-Calatrava[1]

Correspondence
Olivier Terrier
olivier.terrier@univ-lyon1.fr
Manuel Rosa-Calatrava
manuel.rosa-calatrava@univ-lyon1.fr

[1]Laboratoire de Virologie et Pathologie Humaine VirPath, Equipe VirCell, Université Claude Bernard Lyon 1, Université de Lyon, Lyon, France

[2]Laboratoire d'Immunologie, UMR CNRS 7278, INSERM U1095, Faculté de Médecine Timone, Marseille, France

[3]Division of Medical Sciences, Centre for Oncology and Molecular Medicine, University of Dundee, Ninewells Hospital, Dundee, Scotland, UK

While post-transcriptional regulation of gene expression by microRNAs (miRNAs) has been shown to be involved in influenza virus replication cycle, only a few studies have further investigated this aspect in a human cellular model infected with human influenza viruses. In this study, we performed miRNA global profiling in human lung epithelial cells (A549) infected by two different subtypes of human influenza A viruses (H1N1 and H3N2). We identified a common miRNA signature in response to infection by the two different strains, highlighting a pool of five miRNAs commonly deregulated, which are known to be involved in the innate immune response or apoptosis. Among the five miRNA hits, the only upregulated miRNA in response to influenza infection corresponded to miR-146a. Based on a previously published gene expression dataset, we extracted inversely correlated miR-146a target genes and determined their first-level interactants. This functional analysis revealed eight distinct biological processes strongly associated with these interactants: Toll-like receptor pathway, innate immune response, cytokine production and apoptosis. To better understand the biological significance of miR-146a upregulation, using a reporter assay and a specific anti-miR-146a inhibitor, we confirmed that infection increased the endogenous miR-146a promoter activity and that inhibition of miR-146a significantly increased viral propagation. Altogether, our results suggest a functional role of miR-146a in the outcome of influenza infection, at the crossroads of several biological processes.

INTRODUCTION

Influenza viruses belong to the family *Orthomyxoviridae* of enveloped viruses, containing a segmented genome of negative ssRNA. Among the three influenza types (A, B and C), type A is the most virulent pathogen, which presents a high diversity of subtypes due to the combination of 17 different HA proteins and 10 different NA proteins (Palese, 2007; Tong *et al.*, 2012). Influenza A viruses are responsible for recurrent epidemics and, more rarely, pandemics, as illustrated by the emergence of the H1N1 SOIV reassortant in 2009 (Neumann & Kawaoka, 2011).

Influenza viruses are dependent on numerous host cell functions for their replication (Josset *et al.*, 2008).

Although the role and function of influenza viral proteins have been extensively studied, many questions about the mechanisms underlying virus–host interactions remain unanswered. However, important insights have been achieved within the last decade, notably by extensive functional genomic studies (Fornek *et al.*, 2007). For example, the virulence of the 1918 pandemic H1N1 virus was correlated with an atypical expression of cellular genes involved in immune and inflammatory responses, and cell death (Kash *et al.*, 2006; Kobasa *et al.*, 2007). A similar mRNA profiling approach has highlighted the role of the nuclear factor (NF)-κB signalling pathway upon H5N1 infection (Schmolke *et al.*, 2009). Moreover, we have recently shown, with a panel of different human and avian viruses, that influenza infection results in an overall downregulation of the cellular p53 pathway (Josset *et al.*, 2010; Terrier *et al.*, 2011). However, the molecular

Three supplementary figures and one supplementary table are available with the online version of this paper.

mechanisms explaining such differences in cellular gene expression upon influenza infection remain unknown.

Gene expression can be controlled by different key processes, including post-transcriptional regulation by microRNAs (miRNAs), which are small RNA molecules from 21 to 23 nt. These non-coding small RNAs specifically bind to functional elements located in the 3′ UTR of mRNA targets and repress gene expression, either by inhibiting translation or promoting mRNA degradation through the Dicer pathway (Friedman *et al.*, 2009). miRNAs are involved in a wide range of physiological and pathological processes, including cancer (Bartel, 2009). Numerous reports have shown that miRNAs also play important roles in virus–host interactions, particularly in the immune response to infections (Skalsky & Cullen, 2010). For example, some miRNAs can attenuate viral replication by targeting the type I interferon pathway, as illustrated by the antiviral impact of miR-196 and miR-296 on hepatitis C virus (HCV) replication (Pedersen *et al.*, 2007). Recent reports have focused on different viruses [prototype foamy virus (PFV)-1, vaccinia virus (VV), human immunodeficiency virus (HIV)-1, HCV], suggesting that cellular miRNAs can modulate infection by directly targeting viral genes (Lecellier *et al.*, 2005; Otsuka *et al.*, 2007; Huang *et al.*, 2007; Jopling *et al.*, 2005). Thus, variation in miRNA expression upon viral infection can contribute to the cellular response by targeting both cellular and viral genes.

Similar to several viruses, influenza infection results in modulation of miRNA expression, as suggested by the initial observation that influenza viruses alter the mRNA and protein levels of Dicer, a central miRNA-processing enzyme (Matskevich & Moelling, 2007). Moreover, several high-throughput studies using microarray or deep-sequencing technologies have revealed a systematic modulation of host miRNA expression patterns by influenza viruses of different origin, in different cellular models (avian, murine, primate) (Wang *et al.*, 2009; Li *et al.*, 2010a; Peng *et al.*, 2011; Li *et al.*, 2011). Recently, Loveday *et al.* (2012) identified temporal- and strain-specific molecular signatures of host miRNAs in human lung epithelial cells (A549 cells) infected with H1N1 of swine origin and H7N7 of avian origin influenza viruses. Another study compared cellular miRNA signatures in response to highly pathogenic influenza infection in mice and cynomolgus macaques, suggesting that virulence could be partially dependent on miRNA-mediated deregulation of gene expression involved in inflammation and cell death (Li *et al.*, 2010a; Li *et al.*, 2011). Like other viruses, cellular miRNAs have also been identified that functionally inhibit influenza replication, such as miR-323, miR-491 and miR-654, leading to the degradation of PB1 mRNA of H1N1 SOIV (Song *et al.*, 2010).

While miRNAs have been shown to be involved in influenza replication, only a few studies have further investigated this aspect in a human cellular model infected with human influenza viruses. Here, we performed miRNA global profiling in human lung epithelial cells (A549) infected by two different subtypes of human influenza A viruses (H1N1 and H3N2). We identified a common miRNA signature in response to infection by the two different strains, highlighting a pool of five miRNAs commonly deregulated, known to be involved in the innate immune response and apoptosis. Among the five miRNA hits, the only upregulated miRNA in response to influenza infection corresponded to miR-146a. Based on target prediction and functional analyses, we have shown that miR-146a is localized at the crossroads of several biological processes in influenza-infected cells. Using a reporter assay, we confirmed that infection increases the endogenous miR-146a promoter activity. A specific anti-miR146a inhibitor significantly increased viral yield production. Altogether, our results suggest a functional role of miR-146a in the outcome of influenza infection.

RESULTS

Analysis of global miRNA expression between mock- and influenza-infected A549 cells

To investigate the impact of influenza viral infection on the expression of cellular miRNAs, we performed miRNA global profiling in human A549 lung epithelial cells infected by two different subtypes of human influenza A viruses, A/PuertoRico/8/34 (H1N1) and A/Moscow/10/99 (H3N2). An overview of the experimental strategy is given in Fig. 1(a). A549 cells were either mock infected or infected at an m.o.i. of 1 with H1N1 or H3N2 viruses, and total RNAs were isolated at 24 h post-infection (p.i.). An m.o.i. of 1 was performed to ensure that 100 % of the cells were infected at 24 h p.i. (Fig. S1, available in JGV Online), a strategy that we have previously validated and used for a transcriptional profiling study of infected cells (Josset *et al.*, 2010). The purified RNAs were subjected to reverse transcription using a pool of miRNA reverse transcriptase (RT) primers (Human pool A v2.1; Applied Biosystems) and were subsequently amplified and quantified by RT-qPCR in a *Taq*Man array MicroRNA card (Applied Biosystems). Infections were performed in three independent experiments, and each related RT-PCR to analyse miRNA expression was performed in triplicate.

Using the normalized data, we compared the list of miRNAs detected between the three different infections (mock, H1N1 and H3N2) (Fig. 1b). From the total of 377 miRNAs quantified using the MicroRNA card, the percentage of detected miRNAs was similar between mock-infected (42.7 %) and influenza-infected samples (36 and 40 % for H1N1 and H3N2, respectively). Among the detected miRNAs, different signatures were observed between mock- and influenza-infected samples. A limited number of miRNAs were detected in mock infected only ($n=15$) or in influenza-infected cells only ($n=12$ in both H1N1 and H3N2). For example, miR-629 and miR-96 were
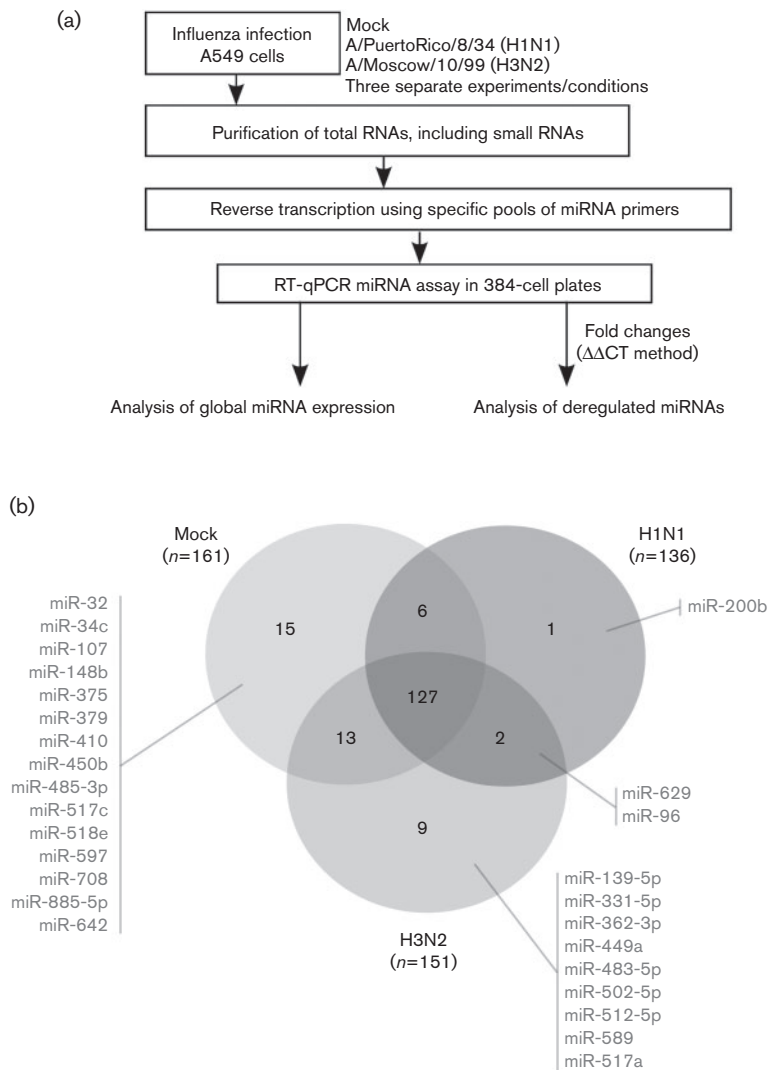
(a)

```
┌─────────────────────┐  Mock
│ Influenza infection │  A/PuertoRico/8/34 (H1N1)
│ A549 cells          │  A/Moscow/10/99 (H3N2)
└─────────────────────┘  Three separate experiments/conditions
           │
           ▼
┌──────────────────────────────────────────────┐
│ Purification of total RNAs, including small RNAs │
└──────────────────────────────────────────────┘
           │
           ▼
┌──────────────────────────────────────────────┐
│ Reverse transcription using specific pools of miRNA primers │
└──────────────────────────────────────────────┘
           │
           ▼
┌──────────────────────────────────────────────┐
│ RT-qPCR miRNA assay in 384-cell plates        │
└──────────────────────────────────────────────┘
      │                        │  Fold changes
      │                        │  (ΔΔCT method)
      ▼                        ▼
Analysis of global miRNA     Analysis of deregulated miRNAs
expression
```

(b)

miR-32
miR-34c
miR-107
miR-148b
miR-375
miR-379
miR-410
miR-450b
miR-485-3p
miR-517c
miR-518e
miR-597
miR-708
miR-885-5p
miR-642

Mock
(*n*=161)

H1N1
(*n*=136)

miR-200b

15   6   1

127

13   2

miR-629
miR-96

9

H3N2
(*n*=151)

miR-139-5p
miR-331-5p
miR-362-3p
miR-449a
miR-483-5p
miR-502-5p
miR-512-5p
miR-589
miR-517a

Fig. 1. Global miRNA expression analysis reveals particular cellular miRNA expression signatures in A549 cells. (a) Schematic representation of the experimental strategy used in this study. (b) Venn diagram for the global expression of cellular miRNAs (mock versus H1N1/H3N2). The number of miRNAs detected for each experimental condition and miRNAs of interest are listed.

only detected in H1N1- or H3N2-infected cells and not in mock-infected cells (Fig. 1b). In contrast, miR-34c and 14 other miRNAs were only detected in non-infected cells (Fig. 1b). Therefore, the majority of expressed miRNAs were commonly detected between the different experimental conditions (n=127, 33.7 % of total miRNAs studied, Fig. 1b). However, their detection levels were different between conditions, indicating that miRNA expression was specifically altered in response to infection.

Cellular miRNA signatures in response to influenza H1N1 and H3N2 infection in human A549 cells

The list of deregulated miRNAs at 24 h p.i. was restricted by two criteria: a fold change threshold of 1.5 (fold change $\leqslant -1.5$ or $\geqslant 1.5$) and a nominal P-value cut-off of 0.05 over the mock-infected miRNA sample (Fig. 2a). A total of 39 and 10 deregulated miRNAs were discriminated by this approach for H1N1 and H3N2, respectively (Fig. 2a). Interestingly, the majority of these miRNAs were downregulated and

corresponded to more than 97 % of the total differentially expressed miRNAs for H1N1 (n=38) and 70 % for H3N2 (n=7) (Fig. 2b). A subset of five miRNAs was commonly and similarly deregulated upon H1N1 and H3N2 infection, including miR-21, miR-29a, miR-29b, miR-146a and miR-452. Among them, only miR-146a was upregulated (Fig. 2a, b).

To validate our results, we performed a comparative RT-qPCR analysis for two distinct miRNAs, using a specific set of primers and the same experimental conditions (A549 cells, m.o.i. of 1, 24 h p.i.), We chose two miRNAs from our global approach with characteristic deregulated profiles in cellular miRNA signatures: let-7f, which was downregulated only in H1N1-infected cells; and miR-146a, which was upregulated in both H1N1- and H3N2-infected cells (Fig. 2b). We determined the mean fold change in three independent experiments for each miRNA, compared with that for mock-infected controls, and data were subjected to statistical analysis (t-student) (Fig. 2c). For let-7f, a significant downregulation was observed in H1N1
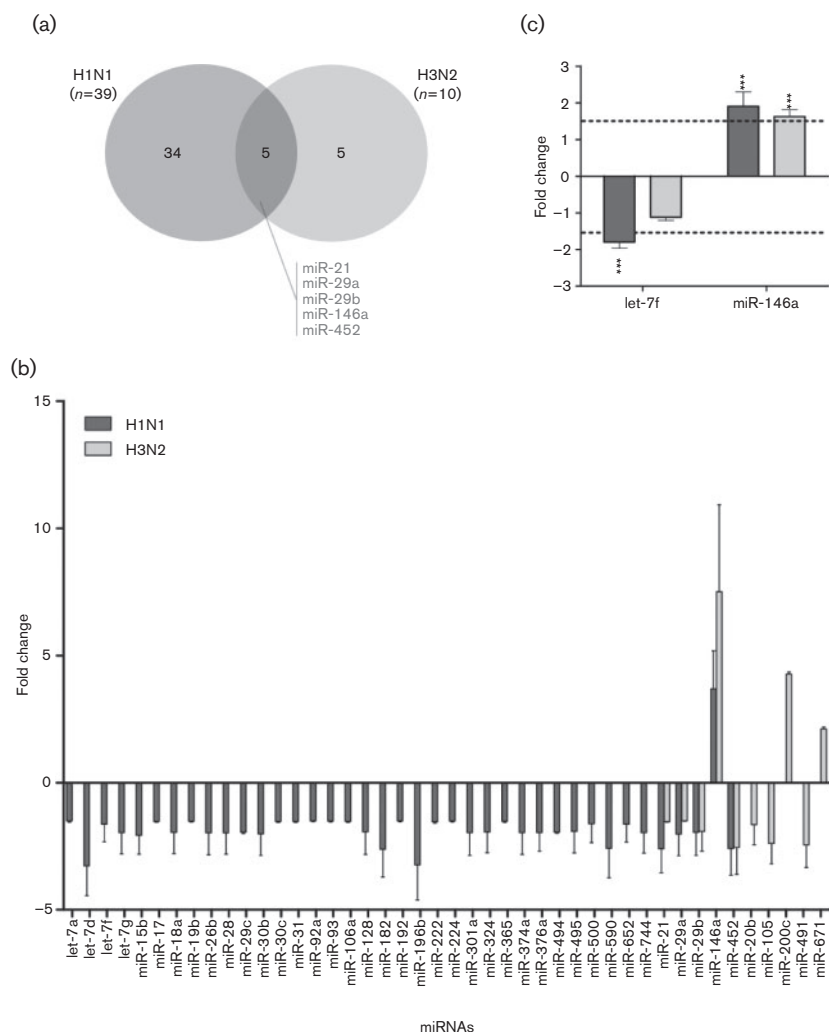
Fig. 2. Commonly deregulated cellular miRNAs in influenza-infected cells are known to be involved in the innate immune response or apoptosis. (a) Venn diagram displaying the list of deregulated miRNAs in influenza-infected cells (H1N1 versus H3N2). (b) Validation by RT-qPCR for let-7f and miR-146a. Fold changes are relative to mock-infected A549 cells. Of the 44 deregulated miRNAs, only five are common to both H1N1 and H3N2 viral infections [highlighted in grey in (a)]. (c) Fold changes relative to mock-infected cells for all deregulated miRNAs in influenza H1N1- and H3N2-infected cells. ***P-value <0.001. Values are means ± SD. Bars: dark grey, H1N1; light grey, H3N2.

(fold change of −1.79, P-value ≤0.001, Fig. 2c), although not in H3N2-infected cells, which was consistent with that observed in the miRNA analysis (Fig. 2b). Similarly for miR-146a, a consistent upregulation was observed in both H1N1- and H3N2-infected cells, with fold changes of 1.91 (P-value ≤0.001) and 1.63 (P-value ≤0.001), respectively (Fig. 2c). These results support the MicroRNA *Taq*Man array results and validate the cellular miRNA signature observed upon influenza infection, determined by our global approach (Fig. 2c).

Upregulation of miR-146a upon infection affects several biological processes

We validated the upregulation of miR-146a by retrieving its known and predicted targets from our previously published dataset of cells infected by influenza, in similar experimental conditions (Josset *et al.*, 2010). Among 65 potential miR-146a target genes, we found 16 of them associated with a significant down-modulation (<−1.5) within the cellular gene expression signature of infection, at least for one viral subtype (Table 1), supporting a strong concordance between

miRNA signatures and previously validated transcriptomic signatures in similar infection conditions.

In order to predict the potential consequences of miR-146 modulation by influenza viruses, we identified the pathways in which these 16 target genes are involved, using MiMI Cytoscape plugin to retrieve all their first-level protein interactants. We obtained a graph composed of 145 nodes (genes) and 493 edges (interactions) (Fig. S2). The functional analysis performed on these 145 genes revealed several key biological processes which might be targeted during influenza infection through the upregulation of miR-146: innate immune response (Fig. 3g, h), pro-inflammatory cytokine production (Fig. 3a), signal transduction (Fig. 3c, e), modulation of transcriptional activity (Fig. 3d, f) and apoptosis (Fig. 3b). All these biological processes are key pathways known to be altered upon influenza infection.

miR-146a plays an antiviral role during influenza infection

To confirm whether the expression of miR-146a, the only upregulated miRNA in both H1N1- and H3N2-infected cells,

Table 1. Gene expression data for the 16 miR-146a target genes down-modulated after influenza infection

Data were extracted from a previously published dataset of cells infected by influenza viruses, with similar experimental conditions (Josset *et al.*, 2010) and constituted the starting point of our bioinformatic analysis. FC, fold change.

Gene		FC	
Abbreviation	Full name	H1N1	H3N2
ABL2	v-abl Abelson murine leukaemia viral oncogene homologue 2	−1.9	−1.4
BCL11A	B-cell CLL/lymphoma 11A (zinc finger protein)	−1.7	−1.2
BCORL1	BCL6 corepressor-like 1	+1.1	−1.9
CARD10	Caspase recruitment domain family, member 10	+1.2	−4.1
DNPEP	Aspartyl aminopeptidase	−1.1	−2.3
FLOT2	Flotillin 2	−1.3	−4.3
GALNT10	UDP-*N*-acetyl-alpha-D-galactosamine : polypeptide *N*-acetylgalactosaminyltransferase 10 (GalNAc-T10)	−1.9	−1.1
IRAK-1	Interleukin-1 receptor-associated kinase 1	−1.4	−2.7
JMJD3	Lysine (K)-specific demethylase 6B	−2.3	+2.9
KBTBD3	Kelch repeat and BTB (POZ) domain containing 3	−1.5	+2.5
LFNG	LFNG *O*-fucosylpeptide 3-beta-*N*-acetylglucosaminyltransferase	−1.3	−1.9
SLC2A3	Solute carrier family 2 (facilitated glucose transporter), member 3	−1.5	+1.1
STRA13	Stimulated by retinoic acid 13 homologue (mouse)	−3.0	−2.2
STRBP	Spermatid perinuclear RNA-binding protein	−1.0	−1.5
SYT1	Synaptotagmin I	+1.4	−2.1
ZNF532	Zinc finger protein 532	−1.1	−2.2

is modulated during the time course of influenza infection, we performed luciferase assays. Using a pGL3basic : miR146aprom luciferase reporter plasmid, whereby the relative luciferase activity directly reflects the miR-146a promoter activity (Taganov *et al.*, 2006; Pichler *et al.*, 2008), we monitored miR-146a promoter activity during the time course of infection of A549 cells by influenza viruses H1N1 and H3N2, with the same m.o.i. used previously, between 0 and 48 h p.i. (Fig. 4). For both viruses, the relative luciferase activity in infected cells significantly increased from 24 h p.i. compared with the activity observed in mock-infected cells, and continued to increase until 48 h p.i. (Fig. 4).

To further explore the role of miR-146a in the influenza viral cycle, we used a commercially available anti-miR-146a inhibitor (Ambion). A549 cells were transfected with either the anti-miR-146a inhibitor (miR-146a inh.) or an anti-miR negative control inhibitor (non-specific inh.). The efficiency of inhibition was evaluated by RT-qPCR 48 h post-treatment, indicating a significant inhibition in miR-146a expression by more than 80 % (Fig. 5a). At this time, treated cells were then infected at an m.o.i. of 1 with influenza virus H3N2, and protein lysates were harvested 24 h p.i. (Fig. 5b). In the absence of miR-146a inhibition, the protein level of a representative miR-146a target gene, interleukin-1 receptor associated kinase 1 (IRAK-1) (Table 1), decreased in infected cells compared with the level in mock. After treatment with anti-miR-146a inhibitor we observed a clear increase of IRAK-1 protein levels in all cases, and an increase of NS1 protein levels, compared with levels of the control (Fig. 5b). Alternatively, cells were infected at an m.o.i. of 0.0001 and harvested 36 h p.i. to quantify virus production by titration. The level of H1N1 or H3N2 infectious viruses produced at

36 h p.i. was significantly higher in anti-miR-146a inhibitor-treated cells compared with their levels in the non-specific inhibitor-treated cells. In H3N2-infected cells, the viral titre was increased by 1 $\log_{10}$, with a $TCID_{50}$ $ml^{−1}$ of 3.7 $\log_{10}$ for the non-specific inhibitor versus 4.7 $\log_{10}$ for the miR-146a inhibitor (Fig. 5c, upper panel). This result was confirmed by Western blot, as a higher level of influenza protein NS1 was observed in anti-miR-146a-treated cells than in non-specific inhibitor-treated cells (Fig. 5c, lower panel), similar to that observed in Fig. 5(b). Altogether, these results show that the inhibition of miR-146a expression increases influenza viral production, suggesting a determinant role of miR-146a in limiting influenza propagation.

DISCUSSION

This study aimed to determine whether cellular miRNAs play a role in human cells infected by influenza viruses of human origin. In addition, we explored factors regulating gene expression to better understand the impact of influenza infection on gene expression previously described in our transcriptomic profiling studies (Josset *et al.*, 2010; Terrier *et al.*, 2011). For this purpose, we performed global miRNA profiling in human lung epithelial cells infected by two different subtypes of human influenza viruses (H1N1 and H3N2).

Global miRNA expression analysis reveals particular cellular miRNA expression signatures in A549 cells

Before our attention directly focused on differentially expressed cellular miRNAs, we analysed the different
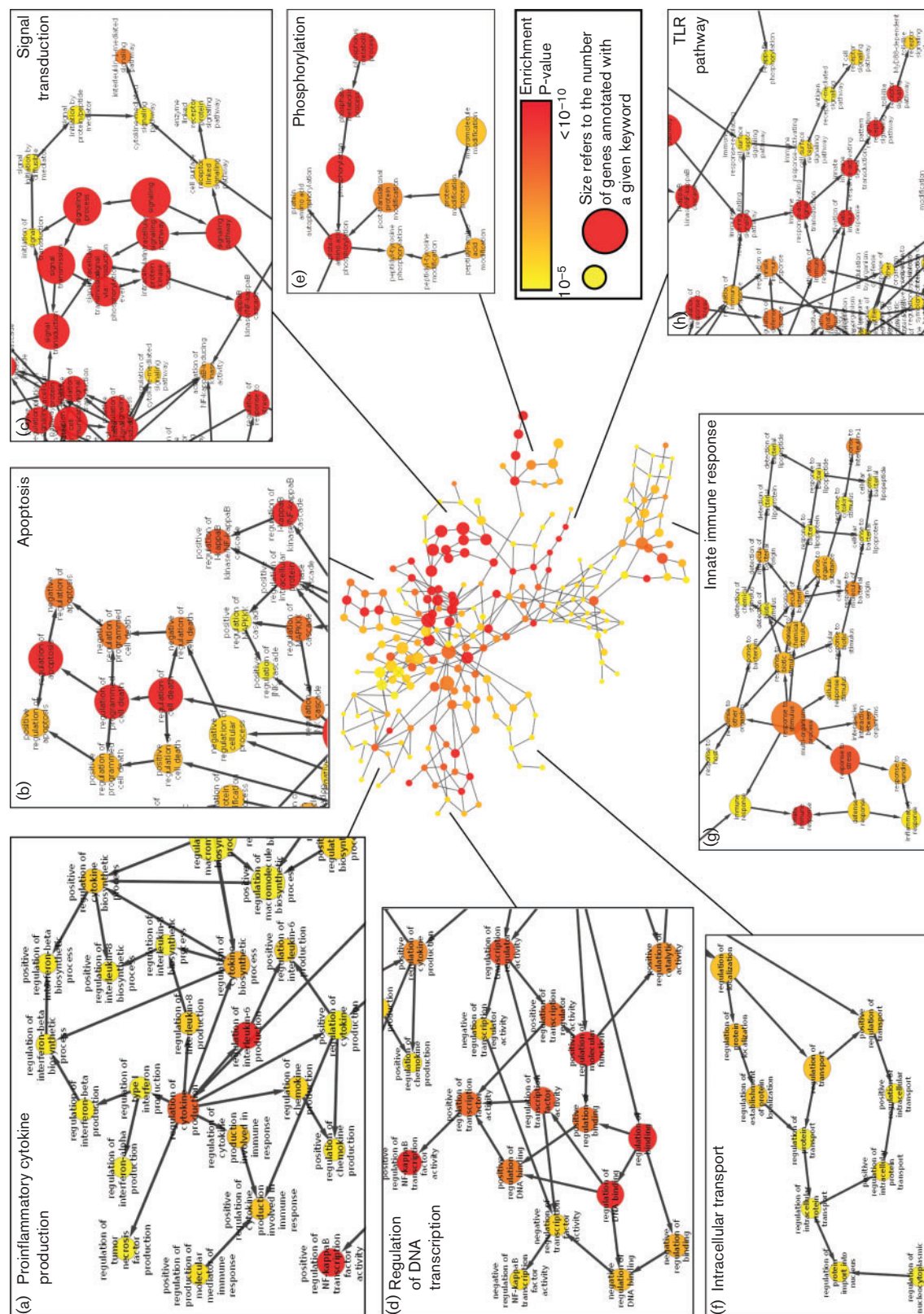
Fig. 3. miR-146a at the crossroads of several biological processes in influenza-infected cells. Functional analysis performed on 145 first-level interactants of miR-146a target genes downregulated during H1N1/H3N2 influenza viral infection, indicating the key biological processes that might be targeted during influenza infection through the upregulation of miR-146: innate immune response (g, h), pro-inflammatory cytokine production (a), signal transduction (c, e), modulation of transcriptional activity (d, f) and apoptosis (b). TLR, Toll-like receptor.
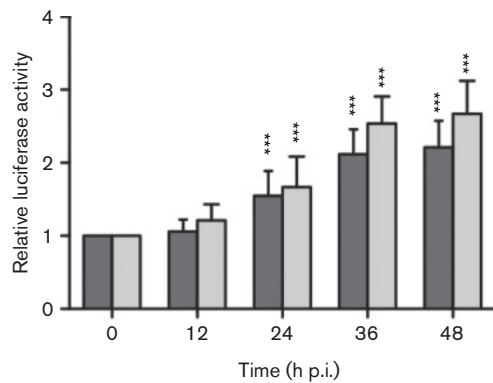
Fig. 4. Analysis of miR-146a promoter activity. The activity assay was performed using a pGL3basic : miR146aprom luciferase reporter plasmid. Luciferase activity was measured at 12, 24, 36 and 48 h p.i. by influenza virus H1N1 or H3N2, and data were normalized to protein concentration and renilla activity for each well. Values are given as multiples of the mock control ($T=0$) and are means ± SD from triplicate measurements in two separate experiments. Data were subjected to a statistical analysis (t-student test) and a significant difference was reached with a P-value <0.05 (***P-value <0.001). Bars: dark grey, H1N1; light grey, H3N2.

Fig. 5. Inhibition of miR-146a expression increases influenza viral production. (a) Efficiency of miR-146a inhibition of expression. Anti-miR-146a inhibitor (miR-146a inh.) or anti-miR negative control inhibitor (non-specific inh.) were transfected in A549 cells. Forty-eight hours after treatment, the efficiency of inhibition was evaluated after RNA extraction and a specific RT-PCR for miR-146a. (b) Anti-miR inhibitor-treated cells were infected at an m.o.i. of 1 for 24 h with influenza virus A/Moscow/10/99 (H3N2). Total protein lysates were subjected to Western blotting for IRAK-1 and NS1 protein levels. (c) Anti-miR-146a inhibitor-treated cells were infected at an m.o.i. of 0.0001 with influenza virus A/PuertoRico/9/34 (H1N1) or A/Moscow/10/99 (H3N2). Viral supernatants and total protein lysates were subjected to the determination of viral titres ($\log_{10}$ TCID$_{50}$ ml^{-1}) and Western blot, respectively. All data were subjected to a statistical analysis (t-student test) and a significant difference was reached with a P-value <0.05 (**P-value <0.005, ***P-value <0.001). Values are means ± SD.

expression patterns between mock-, H1N1- and H3N2-infected cells. Some miRNAs were specifically detected in mock-infected cells but not in infected cells (Fig. 1b). Among these, a member of the miR-34 family, miR-34c, is of particular interest since it is known to be directly regulated by p53 and involved in the regulation of p53-mediated cell death (Hermeking, 2010). Interestingly, we have previously shown, by a transcriptional profiling approach, that members of the p53 pathway, including p53 transcriptional targets, are strongly downregulated upon infection (Terrier *et al.*, 2011). The absence or presence of miR-34c in influenza-infected cells, at levels below the detection threshold, could play a role in p53-mediated cell death upon infection and requires further investigation. This hypothesis is reinforced by the downregulation of miR-34a, another member of the miR-34 family, observed in infected cells (data not shown, fold change just below the 1.5 cut-off). On the other hand, some miRNAs were only detected in H1N1- and/or H3N2-infected cells. For example, miR-200b was only detected in H1N1-infected cells (Fig. 1b). Interestingly, this miRNA was identified by Li *et al.* (2010a) for its high abundance in mice lung tissues and appeared to be differentially deregulated upon infection by two different H1N1 influenza viruses (r1918 and Tx/91).

Commonly deregulated cellular miRNAs in influenza-infected cells are known to be involved in the innate immune response or apoptosis

The analysis of differentially expressed cellular miRNAs upon infection revealed that the majority of miRNAs were downregulated (97 and 70 % for H1N1 and H32N,
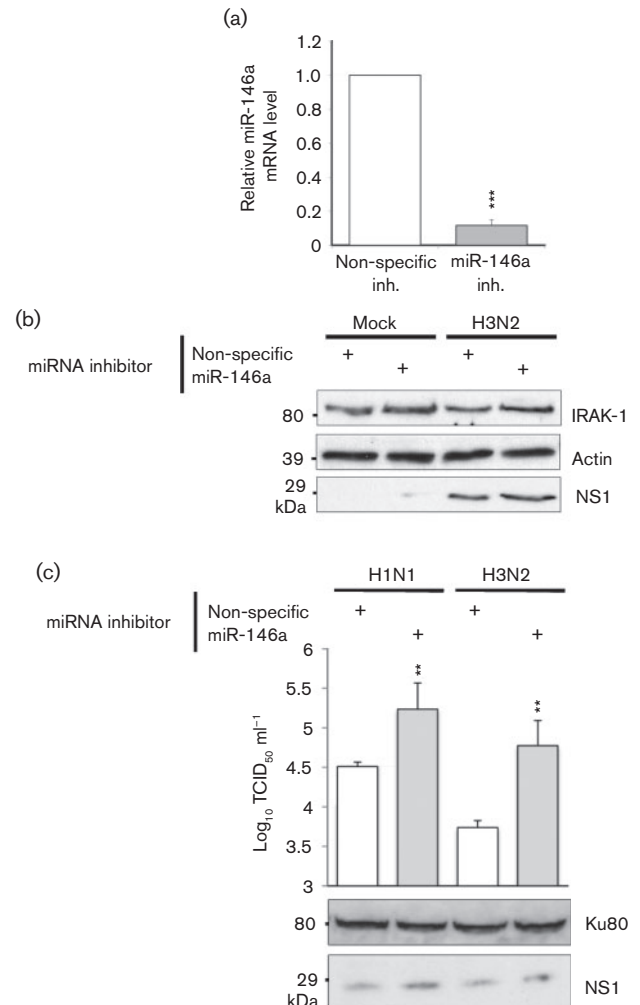
respectively, Fig. 2b). The proportions of up- and downregulated miRNAs appear to be quite different from those described by Loveday *et al.* (2012) at 24 h p.i., with similar infection parameters, although they used a different viral strain (SOIV pandemic H1N1). However, it is difficult to

directly compare these results, as different panels of miRNAs were studied in different arrays. Moreover, the proportion of up- and downregulated miRNAs during the time-course of infection appeared to be dependent on several parameters, such as viral kinetics and nature of the viral strains (Li et al., 2010a; Loveday et al., 2012).

A total of five common miRNAs deregulated upon infection were identified in our analysis: four of them were downregulated (miR-21, miR-29a, miR-29b and miR-452) and only one was upregulated (miR-146a). Interestingly, the deregulation of miR-21, miR-29a, miR-29b and miR-146a in influenza-infected cells has already been described in previously published studies, despite different models and viral strains, highlighting their relevance in the context of influenza infection (Li et al., 2010a; Loveday et al., 2012; Wang et al., 2012). miR-29a and miR-29b have been shown to be downregulated in the lungs of mice infected by different influenza H1N1 strains (Li et al., 2010a) and in A549 cells infected by influenza H1N1 and H7N7 strains (Loveday et al., 2012). Interestingly, in accordance with our results, miR-146a was recently shown to be deregulated in influenza-infected human lung A549 cells (Buggele et al., 2012) and was also characterized as a potential candidate miRNA involved in regulating the host response to avian influenza virus infection in the lungs of broiler chickens (Wang et al., 2012). In addition, it is important to note that the five common deregulated miRNAs revealed in our study, and also characterized by other studies (except for miR-452), are known for their roles in either the immune response (miR-21, miR-29a, miR-146a) or cell death (miR-29b) (Wang & Lee, 2009; Tsitsiou & Lindsay, 2009). Moreover, the deregulation of some of these miRNAs has also been described for other viruses and is summarized in Table S1. Altogether, these results suggest a conserved role for miR-21, miR-29a, miR-29b, miR-452 and miR-146a in the regulation of influenza–host interactions.

miR-146a at the crossroads of several biological processes in influenza-infected cells

The role of miR-146a, the only upregulated miRNA in both H1N1- and H3N2-infected cells, was investigated in more detail. This particular miRNA has been shown to be involved in different human diseases (Li et al., 2010b). More particularly, miR-146a appears to be a negative regulator of the innate immune and inflammatory responses, in a negative feedback regulation loop including IRAK-1 (Fig. 5b), tumour necrosis factor receptor-associated factor 6 (TRAF6) and NFκB, which directly regulates miR-146a. The role of this miRNA was previously investigated in cells infected by different types of viruses [vesicular stomatitis virus, human T-lymphotrophic virus (HTLV) 1, Epstein–Barr virus (EBV)], although not in the case of influenza viruses (Li et al., 2010b; Tsitsiou & Lindsay, 2009). It has been shown that EBV, via LMP1, induces mir146a expression (Cameron et al., 2008). In

addition, miR-146a was recently demonstrated to be induced by HTLV-1 Tax and to increase viral growth (Tomita et al., 2012).

Based on a previously published gene expression dataset, we extracted 16 inversely correlated miR-146a target genes and determined their first-level interactants (Fig. S2). This functional analysis revealed eight distinct biological processes strongly associated with these interactants. Notably, these biological processes were the Toll-like receptor pathway, innate immune response, cytokine production and apoptosis (Fig. 3), which agree with the literature regarding the function of miR-146a in other pathological or physiological contexts (Li et al., 2010b; Tsitsiou & Lindsay, 2009). Moreover, additional biological processes such as signal transduction and intracellular pathways suggest a wider role for miR-146a in the context of influenza infection.

miR-146a, an unexpected role in the antiviral response?

Complementary to this bioinformatic approach, we have observed an increase in miR-146a promoter activity during the time-course of infection using a luciferase assay, supporting an upregulation of miR-14a expression upon influenza expression. In addition, the inhibition of miR-146a expression, using a specific anti-miR inhibitor, was associated with a significant increase in viral production (Fig. 5b, c), suggesting the involvement of miR-146a in the antiviral response. This result was unexpected, considering the known role of miR-146a as an inhibitor of the immune and inflammatory responses and we first anticipated a decrease in viral production. However, since miR-146a is involved in a negative feedback regulation loop with NFκB (Paik et al., 2011), we can hypothesize that the silencing of miR-146a expression leads to an activation of NFκB, which has been shown to promote efficient influenza virus production (Wurzer et al., 2004). However, considering the wide range of biological processes associated with miR-146a upon infection, well-illustrated in our analysis, we cannot exclude other mechanisms for an miR-146a-induced cellular antiviral effect. Interestingly, the upregulation of miR-146a was recently associated with an enhanced immune response observed during co-administration of a split, inactivated influenza H1N1 vaccine antigen with docetaxel (Chen et al., 2012).

Another hypothesis is the possible targeting of viral RNAs by miR-146a. Several reports, from data obtained with different viruses (PFV-1, VV, HIV-1, HCV, influenza viruses), now suggest that cellular miRNAs can regulate infection by directly targeting viral genes (Lecellier et al., 2005; Otsuka et al., 2007; Huang et al., 2007; Jopling et al., 2005; Song et al., 2010; Ma et al., 2012). Recently, in a study focused on miRNA expression in avian influenza-infected chicken lungs, bioinformatic analyses have shown that several miRNAs of interest have putative binding sites in influenza viral genes (Wang et al., 2012). Based on the

sequence data available for the two influenza viruses used in this study, and with the help of target prediction algorithms, we have listed several possible targets in different viral gene segments, such as PB1, PB2 and NP H3N2 for influenza A/Moscow/10/99 (Fig. S3). From these observations, we cannot exclude an antiviral potential for miR146a through inhibition of viral targets, independent of its cellular target, which requires further investigation.

Conclusions and perspectives

Our results have discriminated a short list of miRNAs, which appear to be important regulators in virus–host interactions. Among these, miR-146 was shown to be upregulated during influenza infection similarly to other viruses, and affected viral production, being involved in the antiviral response. The mechanisms behind this unexpected antiviral facet of miR-146a remain to be elucidated and will contribute to a better understanding of influenza–host interactions.

METHODS

Cell lines, viruses and infection. Human lung epithelial A549 cells (ATCC CCL-185) were grown as monolayers in Dulbecco's modified Eagle's medium (DMEM; Gibco), supplemented with 10 % heat-inactivated FBS, 2 mM L-glutamine, 100 U penicillin ml^{-1} and 100 mg streptomycin sulphate ml^{-1} at 37 °C. Influenza viruses A/PuertoRico/8/34 (H1N1), A/Moscow/10/99 (H3N2) were produced in MDCK cells in Eagles's minimal essential medium supplemented with 2 mM L-glutamine, 100 U penicillin ml^{-1}, 100 mg streptomycin sulphate ml^{-1} and 1 mg trypsin ml^{-1}. Viruses were titrated to determine the TCID$_{50}$ in MDCK cells as described in our previous study (Josset *et al.*, 2010). Confluent A549 cells were infected with influenza viruses at an m.o.i. of 1 or 10^{-3} for 1 h in a minimal volume of DMEM supplemented with 2 mM L-glutamine, 100 U penicillin ml^{-1}, 100 µg streptomycin sulphate ml^{-1} and 0.5 µg trypsin ml^{-1} (infection medium) at 37 °C. The cells were then overlaid with fresh infection medium and incubated at 37 °C for 24 h. Viral kinetics for the two different influenza viruses were determined previously (Josset *et al.*, 2010).

RNA extraction and RT-qPCR miRNA assay. Total RNAs, including small RNAs, were isolated using Qiazol reagent (Qiagen) in combination with the miRNAeasy kit (Qiagen) according to the manufacturer's protocol. Purified RNAs were eluted in 30 µl RNase-free water. Reverse transcription reactions contained 390 ng purified RNAs, 1×Megaplex RT primers (Human pool A v2.1; Applied Biosystems), 1×RT buffer, 2.5 mM of each dNTP, 3 mM MgCl$_2$, 1 U µl^{-1} Multiscribe reverse transcriptase (Applied Biosystems) and 0.3 U µl^{-1} RNase inhibitor (Applied Biosystems). The RT reaction mixture had a final volume of 7.5 µl and was incubated for 5 min on ice, followed by 40 cycles (16 °C for 2 min, 42 °C for 1 min, 50 °C for 1 s), 85 °C for 5 min and was then held at 4 °C. The RT products were subsequently amplified with sequence-specific primers contained in a *Taq*Man array MicroRNA card (card A; Applied Biosystems), which enables the simultaneous quantification of 377 different human miRNAs plus several endogenous controls. Six microlitres of RT products was diluted in 444 µl nuclease-free water and was mixed with 450 µl 2× *Taq*Man Universal PCR Master Mix with no Amperase (Applied Biosystems) and was dispensed into the 384 wells by centrifugation. The plates were incubated at 95 °C for 10 min, followed by 40 cycles (95 °C for 15 s, 60 °C for 1 min). The

data were collected and processed using the Plate Utility and Automation Controller software (Applied Biosystems). For each miRNA, the expression level was determined by the 2[-Delta Delta C(T)] method. Data were normalized using the small nucleolar human RNA RNU48 as a control. All experimental conditions were performed in three independent experiments. The list of deregulated miRNAs at 24 h p.i. was restricted by two criteria: a fold change threshold of 1.5 (fold change $\leqslant -1.5$ or $\geqslant 1.5$) and a nominal *P*-value cut-off of 0.05 over the mock-infected miRNA sample (*t*-student test). Comparative RT-qPCR was used to validate miRNA expression changes for let-7f and miR-146a, using the Agilent Mx3005P real-time PCR system (Stratagene; Agilent). Reverse transcription, probes and qPCR primers were used in a *Taq*Man miRNA reverse transcription kit and *Taq*Man miRNA qPCR assays (Applied Biosystems part number 4427975, assay ID 000468 and 000382 for let-7f and miR-146a, respectively). Each miRNA assay was run in three independent experiments. Data are represented as the means ± SD.

Bioinformatic analyses. miRNA targets were retrieved and compiled from TargetScan (Lewis *et al.*, 2005; Grimson *et al.*, 2007). Predicted target gene expression was retrieved from a previous dataset (GEO accession no. GSE22319) (Josset *et al.*, 2010) and analysed using R (version 2.13) and bioconductor libraries. The objective was to determine the biological processes affected by the virally induced upregulation of miR-146a, and for this purpose, the criteria did not need to be too restrictive. Potential target genes for miR-146a are probably differentially regulated by numerous other factors (down- or upregulation), which could be different between H1N1 and H3N2 in terms of nature or kinetics. In this context, we selected all potential target genes with an infected/uninfected ratio below -1.5, at least for one viral subtype, for further analysis. Interactome-based construction of the graph was performed with MiML plugin (Gao *et al.*, 2009). Functional analyses were performed using Gene Ontology Biological Process annotation retrieved through BinGO plugin (Maere *et al.*, 2005). We selected keywords with a Benjamini–Hochberg corrected *P*-value $<1 \times 10^{-5}$. The construction of the interactome graph and the functional enrichment analysis were performed with Cytoscape (version 2.8.2) (Smoot *et al.*, 2011).

miRNA profiling data resource. The data discussed in this publication have been deposited in the NCBI Gene Expression Omnibus (Edgar *et al.*, 2002) and are accessible through GEO Series accession number GSE42003 (http://www.ncbi.nlm.nih.gov/geo/query/acc.cgi?acc=GSE42003).

Analysis of miR-146a promoter activity. The analysis of miR-146a promoter activity was performed using the pGL3basic : miR146aprom luciferase reporter plasmid, which possesses a 558 bp DNA region upstream of the *MIRNA146A* (miR-146a) gene (Taganov *et al.*, 2006; Pichler *et al.*, 2008). Briefly, A549 cells were transfected using Fugene (Promega), following the manufacturer's instructions, with 1 µg reporter construct and 100 ng pRenilla plasmid. After 24 h, transfected cells were infected at an m.o.i. of 1 with influenza virus A/Moscow/10/99 (H3N2). Luciferase activity was measured with the dual-luciferase reporter assay kit (Promega) at 12, 24, 36 and 48 h post-infection, and data were normalized to protein concentration and renilla activity for each well. Values are given as multiples of the mock control (*T*=0) and are means ± SD from triplicate measurements in two separate experiments. Data were subjected to a statistical analysis (*t*-student test) and a significant difference was reached with a *P*-value <0.05.

Inhibition of miR-146a expression. Anti-miR-146a inhibitor or anti-miR negative control inhibitor (Ambion ref AM10722 and AM17010) were transfected into A549 cells using lipofectamine 2000 (Invitrogen), following the manufacturer's instructions. Anti-miR-146a inhibitor is a chemically modified, single-strand nucleic acid

sequence designed to specifically bind to miR-146a. Forty-eight hours after treatment, the efficiency of inhibition was measured after RNA extraction and a RT-PCR specific for miR-146a (Applied Biosystem part number 4427975 assay ID 000382) was performed. Anti-miR-146a inhibitor-treated cells were then infected at an m.o.i. of 1 for 24 h or 0.0001 for 36 h with either influenza virus A/PuertoRico/9/34 (H1N1) or A/Moscow/10/99 (H3N2). Viral supernatants and total protein lysates were subjected to the determination of viral titres and Western blot, respectively. For Western blotting, mouse monoclonal anti-NS1 (Santa Cruz Biotechnology SC-130568) and rabbit polyclonal anti-Ku80 (Cell Signalling no. 2753) and anti-IRAK-1 (Santa Cruz Biotechnology SC-7883) were used. Ku80 was used as a loading control.

ACKNOWLEDGEMENTS

REFERENCES

Bartel, D. P. (2009). MicroRNAs: target recognition and regulatory functions. *Cell* **136**, 215–233.

Buggele, W. A., Johnson, K. E. & Horvath, C. M. (2012). Influenza A virus infection of human respiratory cells induces primary microRNA expression. *J Biol Chem* **287**, 31027–31040.

Cameron, J. E., Yin, Q., Fewell, C., Lacey, M., McBride, J., Wang, X., Lin, Z., Schaefer, B. C. & Flemington, E. K. (2008). Epstein–Barr virus latent membrane protein 1 induces cellular MicroRNA miR-146a, a modulator of lymphocyte signaling pathways. *J Virol* **82**, 1946–1958.

Chen, J., Yuan, L., Fan, Q., Su, F., Chen, Y. & Hu, S. (2012). Adjuvant effect of docetaxel on the immune responses to influenza A H1N1 vaccine in mice. *BMC Immunol* **13**, 36.

Edgar, R., Domrachev, M. & Lash, A. E. (2002). Gene Expression Omnibus: NCBI gene expression and hybridization array data repository. *Nucleic Acids Res* **30**, 207–210.

Fornek, J. L., Korth, M. J. & Katze, M. G. (2007). Use of functional genomics to understand influenza–host interactions. *Adv Virus Res* **70**, 81–100.

Friedman, R. C., Farh, K. K., Burge, C. B. & Bartel, D. P. (2009). Most mammalian mRNAs are conserved targets of microRNAs. *Genome Res* **19**, 92–105.

Gao, J., Ade, A. S., Tarcea, V. G., Weymouth, T. E., Mirel, B. R., Jagadish, H. V. & States, D. J. (2009). Integrating and annotating the interactome using the MiMI plugin for cytoscape. *Bioinformatics* **25**, 137–138.

Grimson, A., Farh, K. K.-H., Johnston, W. K., Garrett-Engele, P., Lim, L. P. & Bartel, D. P. (2007). MicroRNA targeting specificity in mammals: determinants beyond seed pairing. *Mol Cell* **27**, 91–105.

Hermeking, H. (2010). The miR-34 family in cancer and apoptosis. *Cell Death Differ* **17**, 193–199.

Huang, J., Wang, F., Argyris, E., Chen, K., Liang, Z., Tian, H., Huang, W., Squires, K., Verlinghieri, G. & Zhang, H. (2007). Cellular microRNAs contribute to HIV-1 latency in resting primary CD4$^+$ T lymphocytes. *Nat Med* **13**, 1241–1247.

Jopling, C. L., Yi, M., Lancaster, A. M., Lemon, S. M. & Sarnow, P. (2005). Modulation of hepatitis C virus RNA abundance by a liver-specific MicroRNA. *Science* **309**, 1577–1581.

Josset, L., Frobert, E. & Rosa-Calatrava, M. (2008). Influenza A replication and host nuclear compartments: many changes and many questions. *J Clin Virol* **43**, 381–390.

Josset, L., Textoris, J., Loriod, B., Ferraris, O., Moules, V., Lina, B., N'guyen, C., Diaz, J. J. & Rosa-Calatrava, M. (2010). Gene expression signature-based screening identifies new broadly effective influenza A antivirals. *PLoS ONE* **5**, e13169.

Kash, J. C., Tumpey, T. M., Proll, S. C., Carter, V., Perwitasari, O., Thomas, M. J., Basler, C. F., Palese, P., Taubenberger, J. K. & other authors (2006). Genomic analysis of increased host immune and cell death responses induced by 1918 influenza virus. *Nature* **443**, 578–581.

Kobasa, D., Jones, S. M., Shinya, K., Kash, J. C., Copps, J., Ebihara, H., Hatta, Y., Hyun Kim, J., Halfmann, P. & other authors (2007). Aberrant innate immune response in lethal infection of macaques with the 1918 influenza virus. *Nature* **445**, 319–323.

Lecellier, C. H., Dunoyer, P., Arar, K., Lehmann-Che, J., Eyquem, S., Himber, C., Saïb, A. & Voinnet, O. (2005). A cellular microRNA mediates antiviral defense in human cells. *Science* **308**, 557–560.

Lewis, B. P., Burge, C. B. & Bartel, D. P. (2005). Conserved seed pairing, often flanked by adenosines, indicates that thousands of human genes are microRNA targets. *Cell* **120**, 15–20.

Li, Y., Chan, E. Y., Li, J., Ni, C., Peng, X., Rosenzweig, E., Tumpey, T. M. & Katze, M. G. (2010a). MicroRNA expression and virulence in pandemic influenza virus-infected mice. *J Virol* **84**, 3023–3032.

Li, L., Chen, X. P. & Li, Y. J. (2010b). MicroRNA-146a and human disease. *Scand J Immunol* **71**, 227–231.

Li, Y., Li, J., Belisle, S., Baskin, C. R., Tumpey, T. M. & Katze, M. G. (2011). Differential microRNA expression and virulence of avian, 1918 reassortant, and reconstructed 1918 influenza A viruses. *Virology* **421**, 105–113.

Loveday, E. K., Svinti, V., Diederich, S., Pasick, J. & Jean, F. (2012). Temporal- and strain-specific host microRNA molecular signatures associated with swine-origin H1N1 and avian-origin H7N7 influenza A virus infection. *J Virol* **86**, 6109–6122.

Ma, Y. J., Yang, J., Fan, X. L., Zhao, H. B., Hu, W., Li, Z. P., Yu, G. C., Ding, X. R., Wang, J. Z. & other authors (2012). Cellular microRNA let-7c inhibits M1 protein expression of the H1N1 influenza A virus in infected human lung epithelial cells. *J Cell Mol Med* **16**, 2539–2546.

Maere, S., Heymans, K. & Kuiper, M. (2005). BiNGO: a Cytoscape plugin to assess overrepresentation of gene ontology categories in biological networks. *Bioinformatics* **21**, 3448–3449.

Matskevich, A. A. & Moelling, K. (2007). Dicer is involved in protection against influenza A virus infection. *J Gen Virol* **88**, 2627–2635.

Neumann, G. & Kawaoka, Y. (2011). The first influenza pandemic of the new millennium. *Influenza Other Respir Viruses* **5**, 157–166.

Otsuka, M., Jing, Q., Georgel, P., New, L., Chen, J., Mols, J., Kang, Y. J., Jiang, Z., Du, X. & other authors (2007). Hypersusceptibility to vesicular stomatitis virus infection in Dicer1-deficient mice is due to impaired miR24 and miR93 expression. *Immunity* **27**, 123–134.

Paik, J. H., Jang, J. Y., Jeon, Y. K., Kim, W. Y., Kim, T. M., Heo, D. S. & Kim, C. W. (2011). MicroRNA-146a downregulates NFκB activity via targeting TRAF6 and functions as a tumor suppressor having strong prognostic implications in NK/T cell lymphoma. *Clin Cancer Res* **17**, 4761–4771.

Palese, P. (editor) (2007). *Orthomyxoviridae*, 5th edn. Philadelphia, PA: Lippincott Williams & Wilkins.

Pedersen, I. M., Cheng, G., Wieland, S., Volinia, S., Croce, C. M., Chisari, F. V. & David, M. (2007). Interferon modulation of cellular microRNAs as an antiviral mechanism. *Nature* **449**, 919–922.

Peng, X., Gralinski, L., Ferris, M. T., Frieman, M. B., Thomas, M. J., Proll, S., Korth, M. J., Tisoncik, J. R., Heise, M. & other authors (2011). Integrative deep sequencing of the mouse lung transcriptome reveals differential expression of diverse classes of small RNAs in response to respiratory virus infection. *MBio* **2**, e00198-11.

Pichler, K., Schneider, G. & Grassmann, R. (2008). MicroRNA miR-146a and further oncogenesis-related cellular microRNAs are dysregulated in HTLV-1-transformed T lymphocytes. *Retrovirology* **5**, 100.

Schmolke, M., Viemann, D., Roth, J. & Ludwig, S. (2009). Essential impact of NF-kappaB signaling on the H5N1 influenza A virus-induced transcriptome. *J Immunol* **183**, 5180–5189.

Skalsky, R. L. & Cullen, B. R. (2010). Viruses, microRNAs, and host interactions. *Annu Rev Microbiol* **64**, 123–141.

Smoot, M. E., Ono, K., Ruscheinski, J., Wang, P. L. & Ideker, T. (2011). Cytoscape 2.8: new features for data integration and network visualization. *Bioinformatics* **27**, 431–432.

Song, L., Liu, H., Gao, S., Jiang, W. & Huang, W. (2010). Cellular microRNAs inhibit replication of the H1N1 influenza A virus in infected cells. *J Virol* **84**, 8849–8860.

Taganov, K. D., Boldin, M. P., Chang, K. J. & Baltimore, D. (2006). NF-κB-dependent induction of microRNA miR-146, an inhibitor targeted to signaling proteins of innate immune responses. *Proc Natl Acad Sci U S A* **103**, 12481–12486.

Terrier, O., Josset, L., Textoris, J., Marcel, V., Cartet, G., Ferraris, O., N'guyen, C., Lina, B., Diaz, J. J. & other authors (2011). Cellular transcriptional profiling in human lung epithelial cells infected by different subtypes of influenza A viruses reveals an overall down-regulation of the host p53 pathway. *Virol J* **8**, 285.

Tomita, M., Tanaka, Y. & Mori, N. (2012). MicroRNA miR-146a is induced by HTLV-1 tax and increases the growth of HTLV-1-infected T-cells. *Int J Cancer* **130**, 2300–2309.

Tong, S., Li, Y., Rivailler, P., Conrardy, C., Castillo, D. A., Chen, L. M., Recuenco, S., Ellison, J. A., Davis, C. T. & other authors (2012). A distinct lineage of influenza A virus from bats. *Proc Natl Acad Sci U S A* **109**, 4269–4274.

Tsitsiou, E. & Lindsay, M. A. (2009). microRNAs and the immune response. *Curr Opin Pharmacol* **9**, 514–520.

Wang, Y. & Lee, C. G. (2009). MicroRNA and cancer – focus on apoptosis. *J Cell Mol Med* **13**, 12–23.

Wang, Y., Brahmakshatriya, V., Zhu, H., Lupiani, B., Reddy, S. M., Yoon, B. J., Gunaratne, P. H., Kim, J. H., Chen, R. & other authors (2009). Identification of differentially expressed miRNAs in chicken lung and trachea with avian influenza virus infection by a deep sequencing approach. *BMC Genomics* **10**, 512.

Wang, Y., Brahmakshatriya, V., Lupiani, B., Reddy, S. M., Soibam, B., Benham, A. L., Gunaratne, P., Liu, H. C., Trakooljul, N. & other authors (2012). Integrated analysis of microRNA expression and mRNA transcriptome in lungs of avian influenza virus infected broilers. *BMC Genomics* **13**, 278.

Wurzer, W. J., Ehrhardt, C., Pleschka, S., Berberich-Siebelt, F., Wolff, T., Walczak, H., Planz, O. & Ludwig, S. (2004). NF-kappaB-dependent induction of tumor necrosis factor-related apoptosis-inducing ligand (TRAIL) and Fas/FasL is crucial for efficient influenza virus propagation. *J Biol Chem* **279**, 30931–30937.